SYNTHESIS OF METAL-ORGANIC FRAMEWORKS FOR CARBON CAPTURE

An Undergraduate Research Scholars Thesis

by

MARIO NICHOLAS COSIO

Submitted to the Undergraduate Research Scholars program
Texas A&M University
in partial fulfillment of the requirements for the designation as an

UNDERGRADUATE RESEARCH SCHOLAR

Approved by
Research Advisor: Dr. Hong-Cai Zhou

May 2016

Major: Chemistry

TABLE OF CONTENTS

ABSTRACT

Synthesis of Metal-Organic Frameworks for Carbon Capture

Mario Nicholas Cosio
Department of Chemistry
Texas A&M University

Research Advisor: Dr. Hong-Cai Zhou
Department of Chemistry

Current issues at the forefront of environmental concern include problems relating to increased levels of the greenhouse gas CO_2 in the atmosphere. Levels of CO_2 in the atmosphere have reached a historic high and for this reason, researchers have placed much focus on carbon capture and sequestration. Metal-organic frameworks have been studied as a potential solution to this problem. MOFs are a class of highly porous, crystalline material composed of metal nodes and organic linkers that can be engineered to demonstrate carbon capture abilities. One method of designing MOFs with carbon capture ability is the inclusion of Lewis basic groups such as imidazole into the linkers. This work explores the synthesis of MOFs utilizing various linkers containing imidazole to create systems capable of selective absorption of CO_2 at low pressures. Various solvent systems and inclusion of modulating reagents will be explored as new MOF systems are tested.

ACKNOWLEDGMENTS

I would like to acknowledge Stephen Fordham for his mentorship throughout my time with this research group. I would also like to thank Dr. Hong-Cai Zhou for all the opportunities he has provided me with. Last, I would like to thank my family and friends for their continued support in all things I do.

NOMENCLATURE

MOF	Metal-Organic Framework
CCS	Carbon Capture and Sequestration
PCN	Porous Coordination Network
HSAB	Hard-Soft Acid-Base
DMA	N, N-Dimethylacetamide
DMF	N, N-Dimethylformamide
DMSO	Dimethylsulfoxide
PXRD	Poweder X-Ray Diffraction
TBiPP	6,6',6",6"'-(((4Z,6E,9Z,14Z,16E,19Z)-1H,11H-porphyrin-5,10,15,20-tetrayl)tetrakis(benzene-4,1-diyl))tetrakis(imidazo[4,5-f]isoindole-5,7(1H,6H)-dione
PBI	*6,6'-(1,4-phenylene)bis(imidazole[4,5-f]isoindole-5,7(1H, 6H)-dione)*
BPBI	6,6'-(3,3',5,5'-tetramethyl-[1,1'-biphenyl]-4,4'-diyl)bis(imidazo[4,5-*f*]isoindole-5,7(1*H*,6*H*)-dione)
TTI	6,6',6"-(1,3,5-triazine-2,4,6-triyl)tris(imidazo[4,5-*f*]isoindole-5,7(1*H*,6*H*) dione)
SBU	Secondary Building Unit

CHAPTER I

INTRODUCTION

Current problems at the forefront of environmental concern included issues of increased greenhouse gas concentration in the atmosphere, leading to global warming and ocean acidification. The Intergovernmental Panel on Climate Change (IPCC) has reported that it is extremely likely that the climate change we are experiencing is due in part to the rise in the concentration of greenhouse gasses in the atmosphere. Greenhouse gas concentrations in the atmosphere are higher than they have ever been in the history of mankind, global warming trends are unequivocal, and the pH of the world's ocean has increased in acidity by 26%.[1] Of the greenhouse gasses emitted, CO_2 makes up 82.5% of total emission with a majority of the emission coming from fossil fuel combustion for energy production and transportation.[2] For this reason, there is an obvious need to reduce the amount of CO_2 emission in order to help slow climate change.

In order to reduce CO_2 emissions, there has been a recent push for research into the area of carbon capture and sequestration (CCS). Currently, power plants employ amine-scrubbing technologies to capture CO_2 from flue gas before the gas reaches the atmosphere; this process however, is extremely energy and cost demanding and because so, researchers have been searching for alternatives to this method.[3] One possible alternative to amine-scrubbing is the use of porous materials such as activated carbons and zeolite materials. One drawback of activated carbons is their relatively small surface areas, normally between 400~1000 m^2/g. As for zeolites, though they demonstrate selectivity of CO_2 over N_2, they demonstrate poor water stability.[4] For

this reason, this project will explore metal-organic frameworks (MOFs) that can serve as a possible solution to the problems faced by other materials.

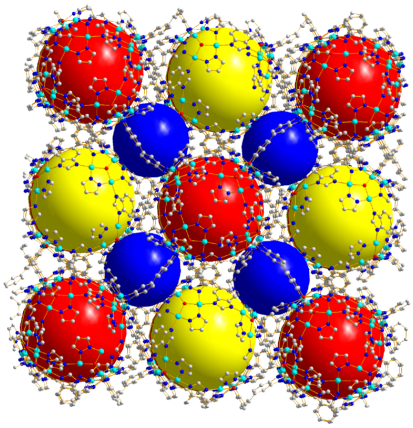

Figure 1. Porous Coordination Network-351, composed of Cu cluster metal nodes and linear, imidazole based linkers.

MOFs are a class of crystalline material known for their high surface areas, permanent porosity, and wide range of applications, including CO_2 capture.[5] MOFs are composed of metal nodes and organic linkers and by rational selection of these components the properties of the bulk material can be tuned.

In addition, experiments can be designed to synthesize MOFs into predetermined shapes in a process called *reticular chemistry.*[6] Much work has been done in the field of characterizing MOF structures into named topologies based off the characteristics of the framework.[7,8] These topologies can then be used to guide the synthesis of future frameworks by rationally selecting materials that will form frameworks with existing topologies. In addition, using Hard-Soft Acid-Base (HSAB) theory, metals can be deliberately selected which will form strong bonds with the coordinating ligands. Imidazole, being an intermediately soft base, will form strong bonds with

intermediately soft acids such as copper, iron, and cobalt and as such these metals will be utilized in this paper.

MOFs work in regions of lower sorption enthalpies than chemical absorption and therefore regenerations are energetically favored.[9] By controlling the composition of the linkers we can also increase the capture ability of the MOFs by increasing the affinity of MOF for CO_2.

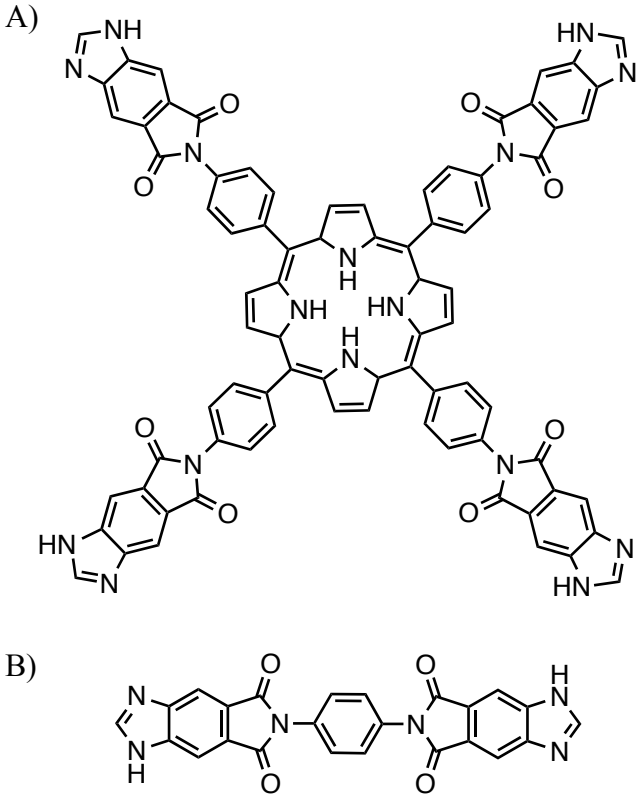

Figure 2. Imidazole based organic linkers. A)TBiPP and B) PBI.

Research has shown that the inclusion of Lewis basic groups into the organic linkers of MOFs can improve the carbon capture abilities of the framework.[10] For this reason, the organic linkers utilized in this project include imidazole-based linkers as seen in Figure 2. In addition to the improved carbon capture ability provided by the imidazole groups, it is expected that the higher

the pKa of the ligand, the stronger the bond between the ligand and metal; imidazole has a pKa of 10.0 and therefore should also form a strong bond with the metal node, adding stability to the framework.[10]

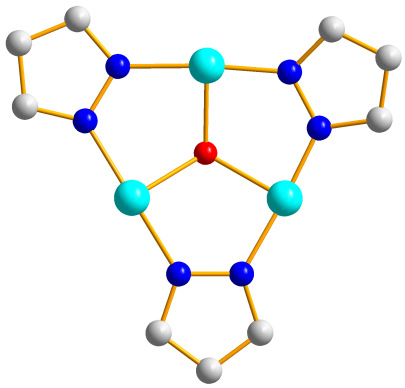

Figure 3. Copper-pyrazole metal cluster

Along with the careful design of the linker, the metal node plays an important part in the synthesis of MOFs with specific properties. The metal node does not need to be a simple metal ion; in fact, metal clusters (Figure 3) along with supermolecular building blocks have been widely used in MOF synthesis because of their functionality.[11] The cluster seen in Figure 4 features open metal sites; when open metal sites were first discovered in MOF-2, it has been found that these sites can increase the packing density of CO_2 due to the coordination of these sites to the oxygen atoms of the CO_2 molecule.[12] Therefore, the use of this trinuclear cluster should allow for an increase in carbon capture ability of the MOF. Improved carbon capture ability is not the only thing changing the metal node of a MOF can affect. Metals like cobalt can impart interesting properties like magnetism into MOF structures[13]; in the work presented, a

MOF is synthesized with a cobalt node in hopes that magnetic properties will be imparted onto the MOF.

The following experiments will be focused on the synthesis of imidazole metal-organic frameworks for carbon capture.

CHAPTER II

METHODS

General information about chemicals used

All commercial chemicals were used as purchased.

Instrumentation used for characterization

A Mercury 300 spectrometer was used to collect all nuclear magnetic resonance spectra. Powder X-ray Diffraction spectra were collected on a BRUKER D8-Focus Bragg−Brentano X-ray powder diffractometer.

Ligand synthesis

Synthesis of 6,6',6'',6'''-(((4Z,6E,9Z,14Z,16E,19Z)-1H,11H-porphyrin-5,10,15,20-tetrayl)tetrakis(benzene-4,1-diyl))tetrakis(imidazo[4,5-f]isoindole-5,7(1H,6H)-dione) (TBiPP)

To a solution of acetic anhydride (36 mL) and propionic acid (800 mL) was added 4-nitrobenzaldehyde (33 g, 218 mmol). The solution was brought to reflux and pyrole (15 mL, 231 mmol) was added drop wise and the reaction was refluxed for 30 minutes. The reaction was cooled over night and the product *(4Z,6E,9Z,14Z,16E,19Z)-5,10,15,20-tetrakis(4-nitrophenyl)-1H,11H-porphyrin (TNPP)* was isolated in 15.4% yield (~20 g). A solution of TNPP (2 g, 2.5 mmol) in 100 mL of concentrated HCl (13.1 M) was bubbled with N_2 for 1 hour. Another solution of HCl (140 mL) and $SnCl_2$ (9.0 g, 40 mmol) was bubbled with N_2 for 1 hour. The $SnCl_2$ solution was canulated into the TNPP solution and refluxed at 78°C for 30 minutes under N_2. The resulting solution was then cooled in an ice bath. The solution was neutralized with

degassed NH_4OH (125 mL) injected into the reaction vessel with a syringe. The solution was centrifuged and a green powder was collected. The green powder was washed with NaOH (5%, 200 mL) then water. After washing the sample was dried under vacuum. The product was soxhlet extracted using $CHCl_3$. The extract was rotovapped to ~150 mL then 100 mL of ethanol (95%) was added and the solution was rotovapped to dryness to yield 0.846 g (~40%) of *4,4',4'',4'''-((4Z,6E,9Z,14Z,16E,19Z)-1H,11H-porphyrin-5,10,15,20-tetrayl)tetraaniline (TAPP)***.** TAPP (0.6g, 0.887 mmol) was dissolved in 50 mL of DMA along with 5,6-dicarboxylic acid benzimidazole (0.8 g, 3.88 mmol). The solution was heated over the weekend at 135°C. the product was centrifuged and then washed with hot water, DMF, and ethanol then dried on the vacuum line. The product yielded *6,6',6'',6'''-(((4Z,6E,9Z,14Z,16E,19Z)-1H,11H-porphyrin-5,10,15,20-tetrayl)tetrakis(benzene-4,1-diyl))tetrakis(imidazo[4,5-f]isoindole-5,7(1H,6H)-dione) (TBiPP)* (0.373 g, 31%).

Synthesis of 6,6'-(1,4-phenylene)bis(imidazole[4,5-f]isoindole-5,7(1H, 6H)-dione) (PBI)

P-phenylenediamine (1.50 g, 13.9 mmol) and 5,6-dicarboxlic acid benzimidazole (5.73 g, 27.8 mmol) were reacted in DMF (100 mL) at 135°C overnight. The sample was then washed with hot DMF, hot ethanol, and hot water before being dried on the Schlenk line. Yield (2.58 g, 43%)

Synthesis of 6,6',6''-(1,3,5-triazine-2,4,6-triyl)tris(imidazo[4,5-f]isoindole-5,7(1H,6H) dione)

Melamine (1.50 g, 11.9 mmol) and 5,6-dicarboxylic acid benzimidazole (7.35 g, 35.7 mmol) were reacted in DMF (100 mL) at 135°C overnight. The sample was filtered and washed with hot water and ethanol to remove residual starting material and dried on the Schlenk line. Yield (2.78 g, 36.7%)

Synthesis of 6,6'-(3,3',5,5'-tetramethyl-[1,1'-biphenyl]-4,4'-diyl)bis(imidazo[4,5-f]isoindole-5,7(1H,6H)-dione)

3,3'5,5'-tetramethylbenzidine (3.00 g, 12.4 mmol) and 5,6-dicarboxylic acid benzimidazole (5.14 g, 24.8 mmol) were reacted in DMF (150 mL) at 135°C over night. The reaction was then washed with water and filtered. The resulting powder was then washed three times with water and the dried in the oven. Yield (not recorded)

MOF synthesis

Synthesis of Cu-Porphyrin MOF

$Cu(NO_3)_2$*$2.5H_2O$ (50 mg), TBiPP (10 mg), and Pyrazole (100 mg) were dissolved in 3 mL Dimethylacetamide (DMA) in a 4 mL vial. Acetic acid (3 drops) was added to the solution and the vial was capped and placed in a 100°C oven for 2 days to yield black crystals.

Synthesis of Ni-Porphyrin MOF

$Ni(NO_3)_2$*$6H_2O$ (30 mg), TBiPP (5 mg), and Pyrazole (100 mg) were dissolved in 3 mL Dimethylacetamide (DMA) in a 4 mL vial. Acetic acid (1 drop) was added to the solution and the vial was capped and placed in a 100°C oven for 2 days to yield black, birefringent crystals.

Synthesis of Zn-Porphyrin crystal

$Zn(NO_3)_2$*$6H_2O$ (30 mg) and TBiPP (5 mg) were dissolved in 3 mL dimethylformamide (DMF) in a 4 mL vial. Pyridine (2 drops) was added to the solution and the vial was capped and placed in a 120°C oven for 2 days to yield black, birefringent crystals.

Synthesis of Co-MOF (linear linker)

$Co(NO_3)_2*6H_2O$ (50 mg) and PBI (10 mg) were dissolved in 1 mL Dimethylacetamide (DMA) in a glass tube. The mixture was degassed by two freeze-pump-thaw cycles. The tube was then frozen again in liquid nitrogen and sealed under vacuum then placed in a 120°C oven for 2 days to yield purple, birefringent crystals.

Synthesis of Co crystal (trigonal planar linker)

$Co(NO_3)_2*6H_2O$ (30 mg) and TTI (20 mg) were dissolved in 1 mL DMF in a glass tube. The mixture was degassed by two freeze-pump-thaw cycles. The tube was then frozen again in liquid nitrogen and sealed under vacuum then placed in a 100°C oven for 2 days to yield purple, birefringent crystals.

Synthesis of Fe crystal (trigonal planar linker)

$Fe(NO_3)_2*2.5H_2O$ (15 mg) and TTI (5 mg) were dissolved in 2 mL DMF in a 4 mL vial. The vial was capped and placed in a 100°C oven for 2 days to yield dark, birefringent crystals.

CHAPTER III

RESULTS

Synthesis of porphyrin crystals

In 2015, Liu et al. published a paper featuring PCN-229.[14] This MOF was composed of a zirconium cluster node and a quadratopic porphyrin linker with an **ftw** topology (Figure 4, A).

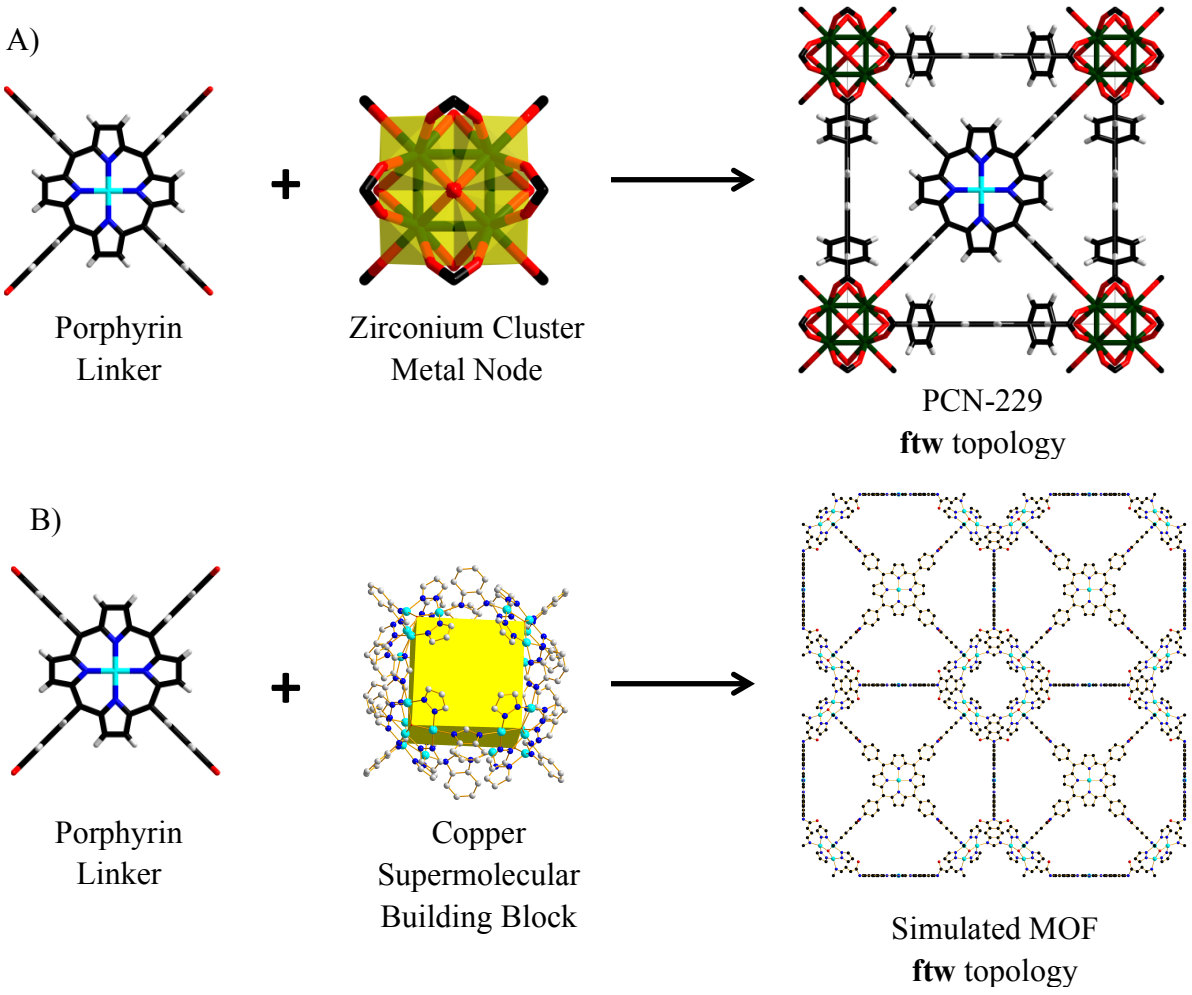

Figure 4. A) PCN-229 is formed from a porphyrin linker and zirconium metal cluster. These materials form a MOF with **ftw** topology. B) A simulated MOF with the same topology as PCN-229 was created utilizing a porphyrin linker and a copper-based supermolecular building block with the same connectivity as the zirconium cluster in PCN-229.

Based off the existence of this MOF system, a simulated MOF with an **ftw** topology, composed of a copper cluster metal node with the same connectivity as the zinc SBU and a tetratopic porphyrin, was composed (Figure 4, B). Various attempts at synthesis of this simulated copper-porphyrin MOF were made using modulating reagents such as pyridine and tetrafluoroboric acid were used to control the kinetic of the reaction, yet the simulated MOF remained elusive. It was not until acetic acid was tested as a modulating reagent that the simulated MOF was finally obtained.

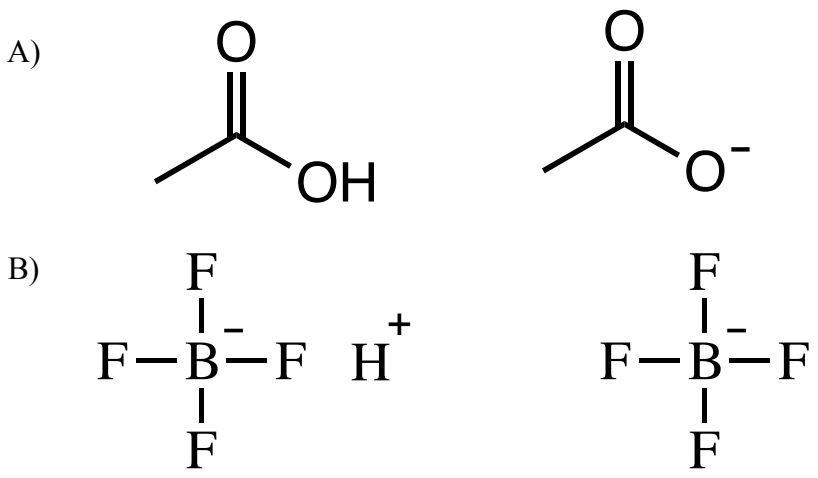

Figure 5. Acid modulating reagents. A) After deprotonation, the acetate ion (right) can serve as a competing linker, slowing the rate of MOF formation. B) After deprotonation, the tetrafluoroborate ion does not act as a competing linker.

MOF formation can be modeled by a reversible ligand substitution reaction. The addition of modulating reagents can assist in the deprotonation of the ligand or hinder it, speeding or slowing the reaction respectively.[15] However, modulating reagents can also affect the reaction in another way. In the case of acetic acid, when the acid deprotonates it becomes a competing acetate ion linker that further slows the reaction (Figure 5, A). The importance of this competing linker can be seen in the case of the copper-porphyrin MOF. In the case of tetrafluoroboric acid,

the modulating reagent is able to slow the deprotonation of the porphyrin linker and therefore slow the reaction but the deprotonated acid does not serve as a competing linker (Figure 5, B). For this reason, it is hypothesized that it is the presence of the competing acetate linker that assists in the formation of the copper-porphyrin MOF.

Powder X-ray diffraction for the new MOF displayed weak peaks. The large amount of void space in the MOF along with the presence of solvent molecules in the pores of the material may be the cause of these weak peaks. A powder pattern was also simulated for the copper MOF which showed the presence of a strong, low angle peak around 2 2θ; an artifact of the powder x-ray instrument that is used to collect the powder pattern of the crystal masks this peak yet it is hypothesized that the intensity of this peak may also mask other peaks present in the powder pattern. A unit cell for the crystal was obtained on a single crystal x-ray instrument along with a single crystal diffraction pattern; this unit cell is in agreement with that of the simulated MOF. Single crystal x-ray data has been obtained for this crystal; however, the crystal structure of the MOF has yet to be obtained.

Along with the crystals, a crust was formed along the edges of the vial (Figure 6). Single crystal diffraction was run on a small sample of the crust and it was found to be amorphous. A method of separation or a new synthesis to avoid the production of this crust must be developed to isolate the crystals before scale up and gas testing can be performed.

Ni and Zn crystals were later synthesized using the same porphyrin linker. Similar to the Cu MOF, the Ni crystal produced weak, low-angle powder peaks due to the large void space of the crystal. Similar to the Cu-porphyrin MOF, the Ni crystal synthesis also formed an amorphous crust on the vial. The amount of Zn crystals produced was small and when run on the powder instrument produced no peaks. This experiment will be run again with more sample to test if low-angle peaks are produced.

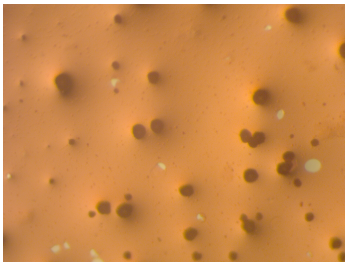

Figure 6. Ni-porphyrin crystals in an amorphous crust.

Multiple trials were run to test if the MOF crystals could be formed without the crust. Various solvents (DMF, DMA, and DMSO) and co-solvents (DMF/MeOH (2:1)) as well as the use of benzoic acid in place of acetic acid were tested in the trial syntheses. None of the trials were a success as either no material would form, an amorphous material would form, or the metal cluster would form instead of the MOF. Hypothesizing that the crust was formed due to the need for nucleation sites, a vial was scratched with a metal spatula and then the reaction was again run. This trial also returned the MOF material with the crust as well. It was concluded that at the moment, the crust is an issue that will remain unsolved.

Synthesis of cobalt crystals

In an attempt to impart magnetic properties in addition to CO_2 capture properties into a MOF, a new MOF with a cobalt node was synthesized. In 2013, Yin et al. published a paper using cobalt and benzo-bis(imidazole).[16] Based off pervious work in which a series of MOFs were constructed by using progressively larger linkers, beginning with benzo-bis(imidazole) (Figure 5, A), it was hypothesized that the same process could be repeated with cobalt. Using PBI (Figure f, B) as a linker, purple crystals of a cobalt MOF were obtained.

When the crystals were synthesized in a capped vial, the crystals were fractured. The cobalt crystals showed a weak powder pattern and the single crystal x-ray diffraction pattern could not be obtained. Based off the color of the crystal some information about its structure can be elucidated. When cobalt displays like a distorted tetrahedron, the color of the MOF will appear purple.[13,16] In an effort to prevent the fracture of the crystals, the reaction was performed again under vacuum in a sealed tube. The crystals harvested by this method returned a strong powder peak at $2\theta < 3$ indicating that the crystal has a large unit cell size and is most likely MOF material; however, the pattern did not provide any other peaks past approximately 3 2θ, the reason as to which still remains unsolved.

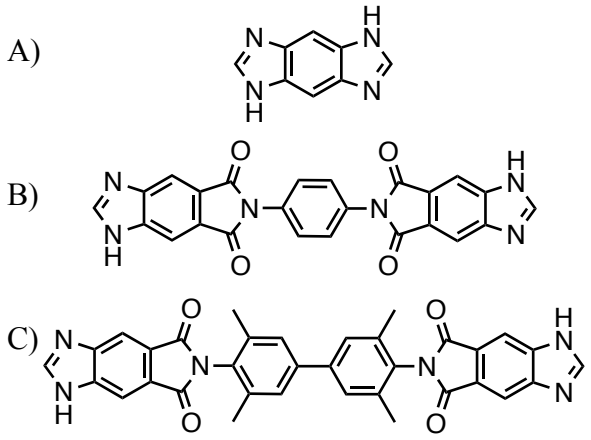

Figure 7. Linkers used in cobalt-crystal synthesis in order of length. A) BBI B) PBI and C) BPBI

In an attempt to synthesize a second cobalt crystal, an extended linker (BPBI) (Figure 8, C) was used under in place of PBI and the reaction was run once again, under the same conditions. What was found was that, as expected, this reaction also returned purple crystals after 2 days in the oven.

Synthesis of crystals with *bor* topology

In 2016, Wang et al published a paper featuring PCN-99 with exhibited a **bor** topology. In order to obtain this topology, a trigonal planar linker and a tetrahedral node were used to construct this framework (Figure 8).[17] Again, using this existing topology as a guide, new crystals were obtained. The linker used was TTI (Figure 9), which, as with the other linkers used in this project, feature imidazole, coordinating groups. The next step in synthesis was to determine what metals would be appropriate for synthesis this framework utilizing HSAB theory and known coordination geometries. This narrowed the possible metal material down to two elements: iron and cobalt.

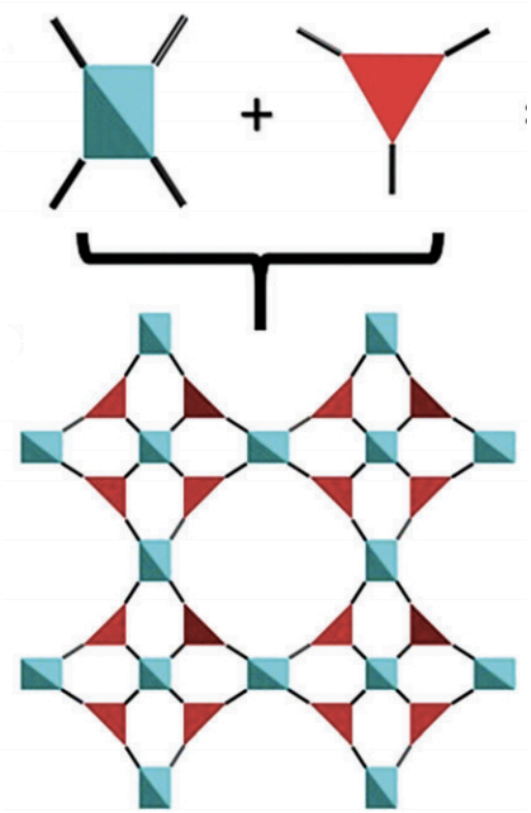

Figure 8. Tetrahedral nodes (blue) and trigonal planar linkers (red) forming the **bor** network topology. Adapted with permission from ref 17. 2016 Royal Society of Chemistry.

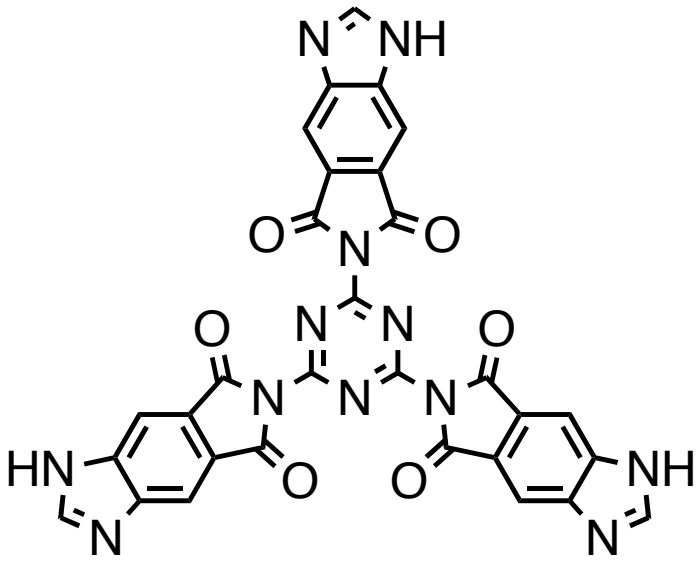

Figure 9. Tritopic TTI linker used in synthesis of new crystals with cobalt and iron metal nodes.

Both metals were used in synthesis of possible frameworks. Cobalt and TTI in DMA produced pink, birefringent crystals. These crystals did not return any power peaks when run on the PXRD instrument, which may be due to the sample decomposing in air as with the purple cobalt crystals previously reported. Iron formed an orange gel with TTI in DMA but change of the solvent system to DMF afforded dark, birefringent crystals. PXRD has not been run on this sample as of yet.

CHAPTER IV

CONCLUSION

The main goal of the project was to develop metal-organic frameworks for carbon capture. As of right now, this project is still ongoing. Various crystals were synthesized using imidazole-based linkers for carbon capture. Now that these crystals have been synthesized testing need to be done on these crystals. Due to foreseen circumstances these tests could not be done in the window for the completion of this thesis; however, the next steps in the project can be discussed.

First, gas studies need to be carried out for each crystal. For each crystal, the BET surface area must be obtained along with CO_2 uptake experiments at low pressures ($P_0/P>1$) and high pressures ($P_0/P<1$). One issue that must be addressed in the area is the separation issue faced with the porphyrin containing materials. If a synthetic route to avoid the formation of the amorphous crust cannot be obtained then an effective means of separating the crust from the crystals must be developed for gas uptake measurements to be accurate. Another issue concerns the fact that the cobalt crystals must be synthesized in sealed tubes and it is hypothesized that these materials may be air sensitive based on the loss of crystalinity overtime. This is a problem as if the crystals must be dried before the studies they will decompose and lose their porosity and gas uptake capacity.

Next, magnetic studies on the cobalt crystals must be completed. The cobalt crystals were synthesized specifically for their magnetic properties; however, there are still problems in this area. Again, the stability of the sample must be addressed if this study is to be performed. If the

sample cannot be prepared for magnetic susceptibility studies, i.e. the sample cannot be dried to determine an accurate mass, then the study cannot be completed. To the knowledge of the author, there is no synthetic method to improve the stability of these crystals so it is unlikely that these results will be obtained in the near future. Also, due to the stability issues of these crystals, it is unlikely that these crystals would be of any use in industrial settings as they would most likely decompose in the conditions of their environment.

Last, this project ended with the synthesis of new crystals of iron and cobalt using a trigonal planar linker. These crystals have yet to be tested for surface area and uptake so it is hard to talk for long about these results. All that can be said is that, if these crystals are in fact MOF material, they are expected to exhibit a **bor** topology, assuming there was no change in oxidation state of the metals or formation of a SBU in situ.

REFERENCES

(1) (IPCC), I. P. o. C. C. *Climate Change 2014: Synthesis Report*, ICPP, 2014.

(2) (USEPA), U. S. E. P. A. *Inventory of U.S. Greenhouse Gas Emissions and Sinks: 1990-2013*, USEPA, 2015.

(3) Rochelle, G. T. *Science* **2009**, *325*, 1652.

(4) Lu, X. J.; Xiao, H. N. *Rev. Adv. Mater. Sci.* **2015**, *42*, 50.

(5) Zhou, H.-C.; Long, J. R.; Yaghi, O. M. *Chem. Rev.* **2012**, *112*, 673.

(6) Yaghi, O. M.; O'Keeffe, M.; Ockwig, N. W.; Chae, H. K.; Eddaoudi, M.; Kim, J. *Nature* **2003**, *423*, 705.

(7) Delgado-Friedrichs, O.; O'Keeffe, M.; Yaghi, O. M. *PCCP* **2007**, *9*, 1035.

(8) Li, M.; Li, D.; O'Keeffe, M.; Yaghi, O. M. *Chem. Rev.* **2014**, *114*, 1343.

(9) Liu, J.; Thallapally, P. K.; McGrail, B. P.; Brown, D. R.; Liu, J. *Chemical Society Reviews* **2012**, *41*, 2308.

(10) Stylianou, K. C.; Queen, W. L. *Chimia* **2015**, *69*, 274.

(11) Guillerm, V.; Kim, D.; Eubank, J. F.; Luebke, R.; Liu, X.; Adil, K.; Lah, M. S.; Eddaoudi, M. *Chem. Soc. Rev.* **2014**, *43*, 6141.

(12) Li, H.; Eddaoudi, M.; Groy, T. L.; Yaghi, O. M. *J. Am. Chem. Soc.* **1998**, *120*, 8571.

(13) Kurmoo, M. *Chem. Soc. Rev.* **2009**, *38*, 1353.

(14) Liu, T.-F.; Feng, D.; Chen, Y.-P.; Zou, L.; Bosch, M.; Yuan, S.; Wei, Z.; Fordham, S.; Wang, K.; Zhou, H.-C. *J. Am. Chem. Soc.* **2015**, *137*, 413.

(15) Feng, D.; Wang, K.; Wei, Z.; Chen, Y.-P.; Simon, C. M.; Arvapally, R. K.; Martin, R. L.; Bosch, M.; Liu, T.-F.; Fordham, S.; Yuan, D.; Omary, M. A.; Haranczyk, M.; Smit, B.; Zhou, H.-C. *Nat Commun* **2014**, *5*.

(16) Yin, X.; Song, Y.; Wang, Y.; Zhang, L.; Li, Q. *Sci. China Chem.* **2014**, *57*, 135.

(17) Wang, X.; Lu, W.; Gu, Z.-Y.; Wei, Z.; Zhou, H.-C. *Chem. Commun.* **2016**, *52*, 1926.